The Preparation of Core-Shell $CaCO_3$ Particles and Its Effect on Mechanical Property of PVC Composites

Ying Xiong, Guangshun Chen, Shaoyun Guo

The State Key Laboratory of Polymer Materials Engineering, Polymer Research Institute of Sichuan University, Chengdu 610065, Sichuan, China

Received 7 September 2005; accepted 1 February 2006
DOI 10.1002/app.24262
Published online in Wiley InterScience (www.interscience.wiley.com).

ABSTRACT: In this study, a novel mechanochemical route to prepare core-shell structured particles was introduced. XPS, TEM, and dissolving experimental results indicate the formation of [(inorganic particle)/(elastomer)] core-shell structured particles, and several kinds of calcium carbonate (nano-$CaCO_3$) particles with various interfaces were obtained. The mechanical properties and morphological results indicate that the surface treatment of nano-$CaCO_3$ particles and the existence of outer elastic layer will strengthen the interfacial interaction between nano-$CaCO_3$ particles and PVC matrix, which results in improvement of mechanical properties of PVC/$CaCO_3$ composites. The theoretical calculations of the interfacial interaction and DMA results confirm these especially when the surface of nano-$CaCO_3$ particles was treated by MMA and coated in succession by ACR through vibro-milling. © 2006 Wiley Periodicals, Inc. J Appl Polym Sci 102: 1084–1091, 2006

Key words:poly(vinyl chloride); core-shell particles; mechanochemistry; mechanical property

INTRODUCTION

Poly(vinyl chloride) (PVC) is a typical example of brittle thermoplastic and many efforts have been made to improve its fracture resistance for several decades. According to existing reports, modifiers for toughening PVC can be divided into three classes: (1) blending with elastomer, for example, acrylonitrile-butadiene rubber, natural rubber, poly(methyl methacrylate-*co*-methacrylate) (ACR), chlorinated polyethylene, poly(methacry-*co*-butylene-styrene);[1–4] (2) blending with short fiber, such as glass fiber, whisker, etc.;[5–8] (3) blending with rigid particles, such as poly(methyl methacrylate) (PMMA), calcium carbonate ($CaCO_3$), and silicon dioxide.[9] These modifiers show various degrees of toughening PVC but there are respective limitations for them when they are used solely, for example, rigid particles can both toughen and reinforce PVC but only to a certain extent, and blending with elastomers can greatly improve the impact resistance of PVC but often results in a great decline of tensile strength, modulus, and heat resistance. So some researchers used both elastomers and rigid particles or short fiber fillers to obtain PVC blends with good performance, and synergic toughening effect was sometimes found.[10–12] Even then, a modifier owning properties of both elastomer and rigid particles is more advantageous in application. Many studies revealed that core-shell structured particles were a good choice for this aim, because these particles can easily own various properties if the materials of core or shell is designed specially. Until now, core-shell particles used as modifiers are generally obtained from seeded emulsion polymerization and the structure of these core-shell particles are often organic core and organic shell.[13–16] Although core-shell particles with inorganic core and organic shell have been prepared by sol–gel process or surface grafting and polymerization,[17,18] preparation of core-shell particles with inorganic core and organic shell prepared in solid is seldom reported and reports about core-shell particles with inorganic core and elastomer shell are also seldom found . Meanwhile, it is well known that solids with activated surfaces can induce various mechanochemical phenomena. Especially, the solid surface has a remarkable reactivity because of the existence of the fresh surfaces and the radical or ion-type active center obtained by vibro-milling the solids. It can be used as grafting supports.[19,20] Through vibro-milling, a homogeneous dispersion of nanoparticles in the matrix can be obtained and aggregation of nanoparticles can be inhibited.[9,12]

In this study, we prepared core-shell structured particles through vibro-milling method in solid in the presence of nano-$CaCO_3$ and ACR. The core is nano-

Correspondence to: Y. Xiong (nic7702@scu.edu.cn).
Contract grant sponsor: National High Technology Research and Development Program of China (863 Program); contract number: 2003AA333010.
Contract grant sponsor: Program for Changjiang Scholars and Innovative Research Team in University.

TABLE I
Surface Treatment of Nano-$CaCO_3$

Sample codes	Treatment mode
$CaCO_3$	Untreated nano-$CaCO_3$
$CaCO_3$–PMMA	Vibro-milling $CaCO_3$ and MMA for 3 h, the weight ratio of $CaCO_3$/MMA is 800/50
$CaCO_3$/ACR	Blending $CaCO_3$ and ACR directly
$CaCO_3$–ACR1	Vibro-milling $CaCO_3$ and ACR for 1 h
$CaCO_3$–ACR2	Vibro-milling $CaCO_3$ and ACR for 2 h
$CaCO_3$–PMMA/ACR	Blending $CaCO_3$-PMMA and ACR directly
$CaCO_3$–PMMA–ACR1	Vibro-milling $CaCO_3$-PMMA and ACR for 1 h
$CaCO_3$–PMMA–ACR2	Vibro-milling $CaCO_3$-PMMA and ACR for 2 h

For all treatment modes above, the weight ratio of ACR/$CaCO_3$ is 20/80, the rotation speed of the vibro-mill is 800 rpm, the ratio of steel ball/nano-$CaCO_3$ (by mass) is about 13/1, the diameter of the steel ball is between 4 and 12 mm, and vibro-milling is carried out under the protection of nitrogen gas.

$CaCO_3$ and the shell is ACR. To reinforce the interfacial interaction between nano-$CaCO_3$ and ACR, $CaCO_3$ is grafted with methyl methacrylate (MMA) by vibro-milling. The characterization of the core-shell structured particle and the effect of core-shell structured particles on mechanical properties and morphology of PVC/nano-$CaCO_3$ composites were studied.

EXPERIMENTAL

Materials

The poly(vinyl chloride) (PVC) used was SG-7 (supplied by Yibing Tianyuan Stock, China) with a number-average molecular weight of 5.0×10^4. The PVC was mixed with 4 phr tribasic lead sulfate, 2 phr dibasic lead phosphite, 1 phr stearic acid, and 0.5 phr oxidized polyethylene wax before use. Tribasic lead sulfate, dibasic lead phosphite, stearic acid, and oxidized polyethylene wax were commercial products. The ACR (KM355P) used was supplied by Rohm and Hass China Pte. Nano-$CaCO_3$ used was supplied by Shandong Shengda nanomaterials, China, with mean particles size ca. 40 nm. MMA used was analytical reagent and washed by alkali liquor and purified by distillation under reduced pressure before use.

Sample preparation

The design of toughening particle needs to take into account a number of general factors. First, it is important to have an outer elastic layer to provide a means of stress transfer from the matrix to the inorganic rigid particles. Second, the interfacial interaction between rigid particles and elastic layer or between elastic layer and the matrix will greatly affect the properties of PVC composites. ACR was chosen as the elastic layer in this study because it is well compatible with PVC. To enhance the interface adhesion between nano-$CaCO_3$ and ACR, MMA was chosen as surface modified agent.

All kinds of nano-$CaCO_3$ particles used in this study were listed in Table I and the weight ratio of nano-$CaCO_3$/ACR is 80/20, the typical mechanochemical preparation of $CaCO_3$-ACR core-shell structured particles was conducted as follows. Above all, nano-$CaCO_3$ was dried at 110°C for 15 h to eliminate possible water absorption and then the desired amount of dried nano-$CaCO_3$ and purified monomer were vibro-milled for 3 h in a vibro-milling machine. Third, ACR was added into the vibro-mill to be covibro-milled for 1 or 2 h before the final core-shell structured particles were taken out.

The sample was prepared by blending PVC with a certain amount (0–15 phr) of nano-$CaCO_3$ particles for a period of 8 min in a twin roll mixer at 170°C and then compression molded at 185°C.

Measurements and characterization

Stress–strain behavior of PVC/nano-$CaCO_3$ composites was measured on an Instron 4302 tensile machine (Canton, MA) with dumb-bell specimen dimensions of $25 \times 6.5 \times 1$ mm^3 and a crosshead speed of 10 mm/min (GB/T 1040–1992). The Izod notched impact strength was measured on a XJ-40A Impact tester (Chengde, China) and conducted according to the regulation mentioned in GB/T 1843–1996. All tests above were carried out at room temperature with six or seven specimens for each sample.

The surface chemical structures of some kinds of $CaCO_3$ particles were observed by an X-ray photoelectron spectrum (XPS) on these $CaCO_3$ particles powders. The morphology of a core-shell structured particle was observed by a transmission electron microscope (TEM) (JEM-CX100, Tokyo, Japan) operated at 100 kV, before observation, the core-shell structured particle powder was scattered in alcohol first and

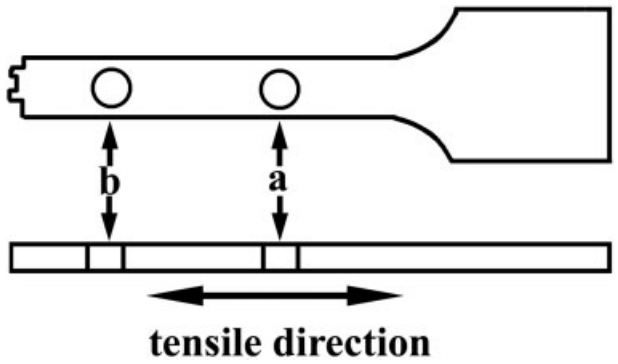

Figure 1 Schematic diagram of longitudinal section of tensile-fractured specimen for SEM observation.

loaded on a special net and dried. On the other hand, a dissolving experiment was carried out to determine whether $CaCO_3$ particles are coated completely or not. The solvent is hydrochloric acid (0.15*N*). Some kinds of $CaCO_3$ particles were weighted (W_1) and dissolved into the hydrochloric acid till there was no gas blowing off, then filtrated, washed, and dried, and weighted insoluble residues (W_2) and percentages (G) of insoluble residues in original particles were calculated as follows: $G = W_2/W_1 \times 100\%$. The phase structure and fractured behavior of the composites were examined by scanning electron microscope (SEM) analysis. For fractured behavior analysis, the tensile fractured surfaces were cut open parallel to tensile direction under liquid nitrogen temperature (see in Fig. 1). For phase structure observation, the impact samples were brittle fractured under liquid nitrogen temperature. The longitudinal sections of the tensile fractured surfaces and the impact fractured surfaces were coated with silver-palladium alloy and examined with a SEM-X650 (Tokyo, Japan) instrument with an accelerating voltage of 20 kV. Two zones of the longitudinal sections were selected for observation as illustrated in Figure 1. The DMA tests were conducted on a DMA-7e (Perkin–Elmer, USA) in a flexural mode (three-point bend) with a frequency of 1 Hz and a heating rate of 2.5°C/min within the range of −50 to 140°C. The specimen dimensions were $20 \times 2.5 \times 4$ mm^3.

RESULTS AND DISCUSSION

Characterization of core-shell structured particles

As shown in Figure 2(a)–2(c), it can be seen that when as a whole $CaCO_3$ particles are treated with different modes, the content of oxygen and calcium of $CaCO_3$ surfaces decrease with the increase of the content of carbon on $CaCO_3$ surface. The peak at 284.8 eV (the C in C—H) is obviously higher than the peak at 289.8 eV (the C in C—O) in the sample of $CaCO_3$–PMMA, while the later is higher in the pure $CaCO_3$, and compared with $CaCO_3$, the area of C peaks of $CaCO_3$–PMMA, $CaCO_3$–ACR1, and $CaCO_3$–PMMA–ACR1 particles increase distinctly, meanwhile the area of O and Ca peaks decrease obviously, indicating that on the surfaces of these $CaCO_3$ particles the contents of carbon increase, while the contents of oxygen and calcium decrease evidently, especially in the sample of $CaCO_3$–PMMA–ACR1, the element of calcium almost disappear.

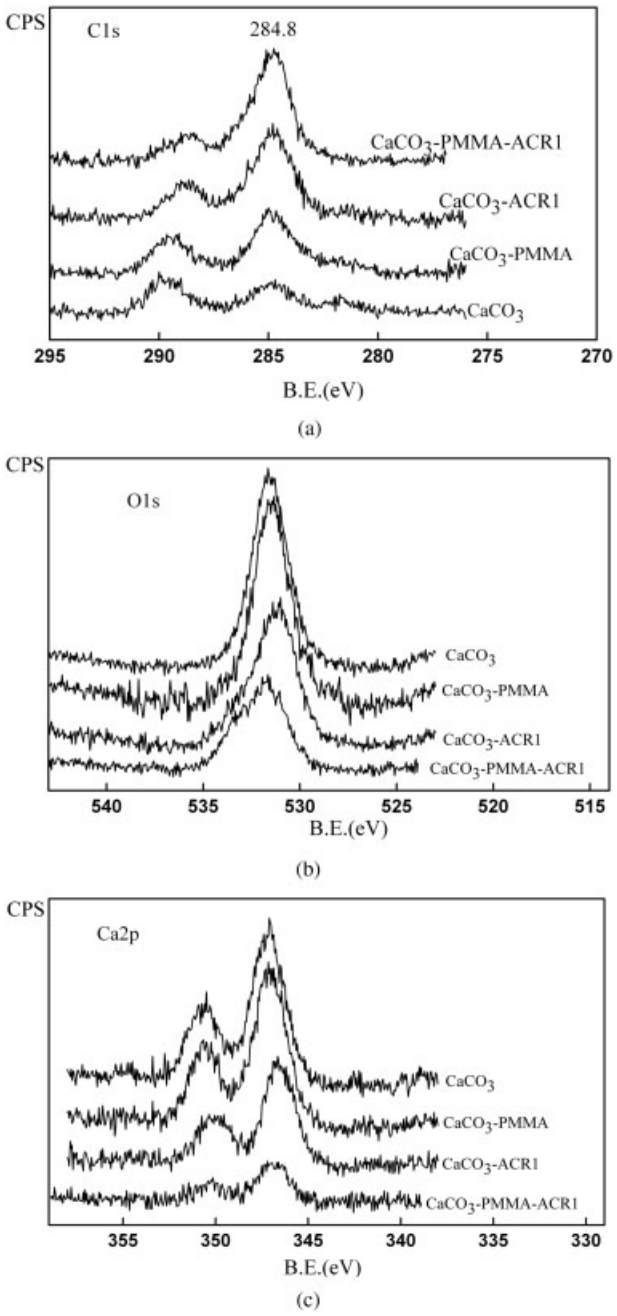

Figure 2 (a) XPS spectra of carbon of different $CaCO_3$ particles; (b) XPS spectra of oxygen of different $CaCO_3$ particles; and (c) XPS spectra of calcium different $CaCO_3$ particles ACR $CaCO_3$–PMMA–ACR1.

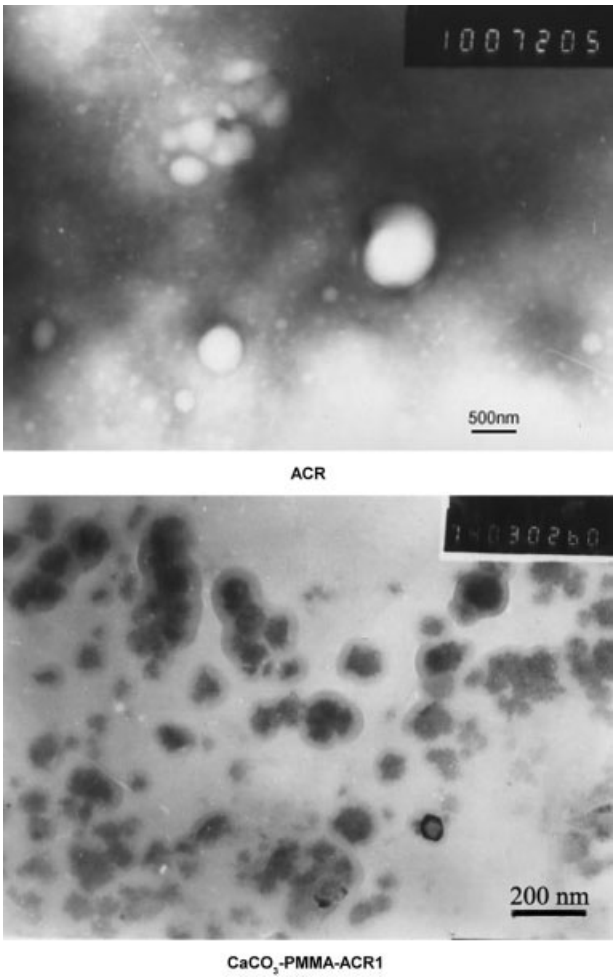

Figure 3 TEM micrographs of ACR and $CaCO_3$–PMMA–ACR1 particle.

All information above demonstrates that MMA can be grafted to the surface of $CaCO_3$ and a large number of $CaCO_3$ has been coated by ACR through vibro-milling. The morphology of ACR and $CaCO_3$–PMMA–ACR1 particles was observed by TEM on ACR and $CaCO_3$–PMMA–ACR1 particles powder respectively, and the result is shown in Figure 3. It can be seen that there was no core in ACR particle and the surface of $CaCO_3$–PMMA–ACR1 particle was different from its inner part. From Table II, it can be seen that percentages of insoluble residues in original particles were much higher than the weight ratio of ACR (20%) in these vibro-milled particles, which indicates that many $CaCO_3$ particles were completely coated by ACR. When the surfaces of $CaCO_3$ particles were grafted by MMA, percentages of insoluble residues in original particles were enhanced. Percentages of insoluble residues in original particles also increased with the increase of vibro-milling time. All these indicated that treatment of surface with MMA and increase of vibro-milling time are beneficial to the formation of core-shell structured particles with complete coat. Combining results of XPS, TEM, and dissolving experiment, it can be said that a core-shell structured particle was obtained by vibro-milling.

Mechanical properties of PVC/nano-$CaCO_3$ composites and interfacial interaction between PVC and nano-$CaCO_3$ particles

The effects of various nano-$CaCO_3$ particles on mechanical properties of PVC/nano-$CaCO_3$ composites are shown in Figure 4(a)–4(b). It can be seen that as a whole the impact strength increases with the addition of various nano-$CaCO_3$ particles, while the tensile strength decreases with the increase of these particles. Meanwhile, comparing PVC/($CaCO_3$/ACR) with PVC/($CaCO_3$–ACR1) and PVC/($CaCO_3$–ACR2), the formation of core-shell structured particles did not result in remarkable change of notched Izod impact strength, although there was a little increase of tensile strength. But comparing PVC/($CaCO_3$–PMMA/ACR) with PVC/($CaCO_3$–PMMA–ACR1), and PVC/($CaCO_3$–PMMA–ACR2), the formation of core-shell structured particles resulted in remarkable increase of notched Izod impact strength and a little increase of tensile strength. All these indicated that the affinity between $CaCO_3$ and ACR is poor; at the absence of PMMA, the core-shell structured particles ($CaCO_3$-ACR1 and $CaCO_3$-ACR2) were easily destroyed and stress cannot be easily transferred to $CaCO_3$ particles. In the presence of PMMA, the interfacial interaction between $CaCO_3$ and ACR was strong so that the core-shell structured particles ($CaCO_3$–PMMA–ACR1 and $CaCO_3$–PMMA–ACR2) can easily transfer stress from outer elastic layers to rigid cores before these particles were destroyed, which makes full use of the synergetic effect of elastomer and rigid particle.

Comparing PVC/($CaCO_3$/ACR) with PVC/($CaCO_3$–PMMA/ACR), it can be seen that grafting PMMA to surface of $CaCO_3$ cannot directly toughen PVC/nano-$CaCO_3$ composites, the reason is that PMMA is more compatible with ACR than PVC, so the grafting PMMA to surface of $CaCO_3$ cannot lead to improvement of interfacial interaction between $CaCO_3$ and PVC.

Comparing PVC/($CaCO_3$–ACR1) with PVC/($CaCO_3$–ACR2) and PVC/($CaCO_3$–PMMA–ACR1)

TABLE II
Results of Dissolving Experiment in Hydrochloric Acid

Sample	*G* (%)
$CaCO_3$	1.42
$CaCO_3$/ACR	19.41
$CaCO_3$–ACR1	37.87
$CaCO_3$–ACR2	44.95
$CaCO_3$–PMMA–ACR1	42.72
$CaCO_3$–PMMA–ACR2	46.77

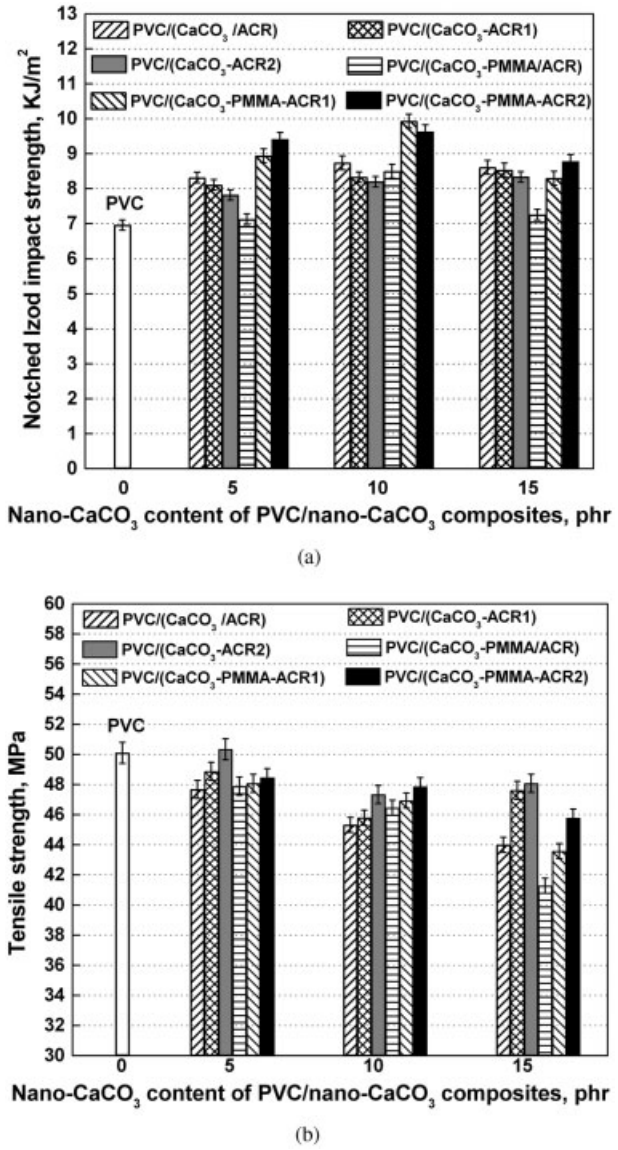

Figure 4 (a) Effect of various nano-$CaCO_3$ particles on notched Izod impact strength of PVC composites and (b) effect of various nano-$CaCO_3$ particles on tensile strength of PVC composites.

with PVC/($CaCO_3$–PMMA–ACR2) respectively, it can be seen that vibro-milling time has a little effect on properties of PVC/nano-$CaCO_3$ composites during experimental vibro-milling time range, but the longer the vibro-milling time is, the more remarkable the aggregation of these nano-$CaCO_3$ particles due to the plastic effect of ACR during vibro-milling.

From all above phenomena, we can draw a conclusion that different interfacial interactions between nano-$CaCO_3$ particles and PVC or ACR were obtained by the methods used, which results in changes of mechanical properties of PVC/$CaCO_3$ composites.

Meanwhile, the characterization of interfacial interaction gets more and more attention. To confirm that the effect of the interfacial interaction on the mechanical property of the composites, a lot of work has been done and some models have been developed to describe the relation between the measured tensile strength and modulus and the interfacial interaction of polymer composites. Yield stress is proved to be an excellent property to predict interfacial interaction quantitatively in heterogeneous polymer systems. Concerning stress concentration, interface adhesion, and dimensional factor of filler, a model[21,22] developed previously described the effect of decreasing load-bearing cross section areas and the interfacial interaction on the yield stress of particulate-filled polymeric system. The expression of yield stress takes the equation as follows:

$$\sigma_c = \sigma_m[(1 - \varphi_f)/(1 + 2.5\varphi_f)] \exp(B_\sigma \varphi_f) \qquad (1)$$

where σ_c and σ_m are the yield stresses of the composite and the matrix respectively, φ_f is the volume fraction of the filler in the composite, and B_σ is the parameter characterizing interfacial interaction. The term (1-φ_f)/(1 + 2.5φ_f) takes into account the decrease of the

TABLE III
B_σ Values from eq. (2) of PVC Composites Filled with Different $CaCO_3$ Particles

Sample	B_σ
PVC/($CaCO_3$/ACR)	1.35
PVC/($CaCO_3$–PMMA/ACR)	1.44
PVC/($CaCO_3$–ACR2)	2.07
PVC/($CaCO_3$–PMMA–ACR2)	2.42

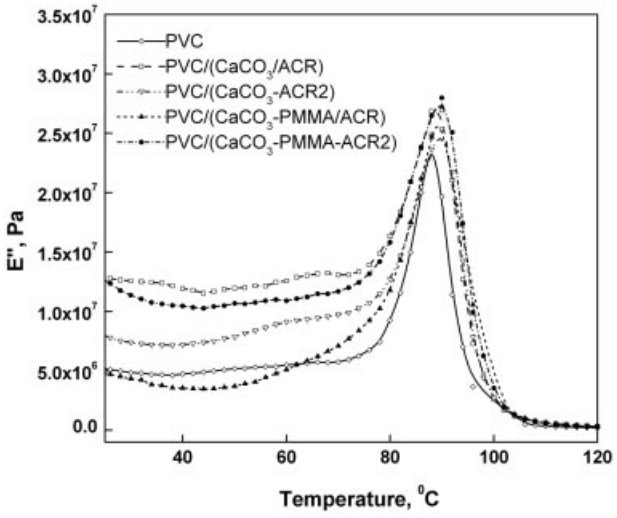

Figure 5 Loss modulus of PVC and various PVC/nano-$CaCO_3$ (100/15) composites.

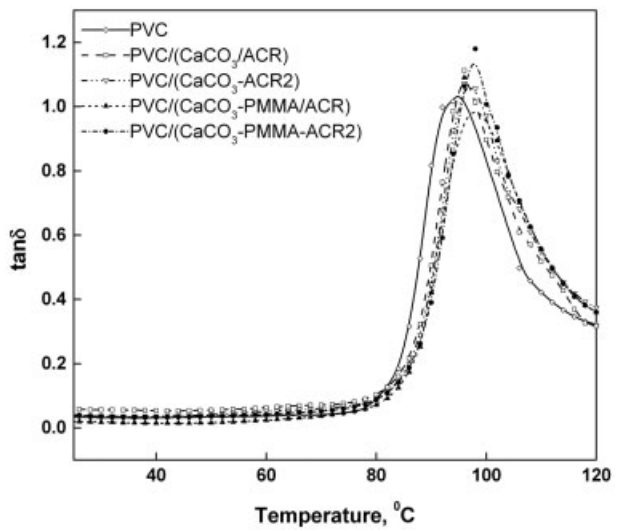

Figure 6 Loss factor (tan δ) of PVC and various PVC/nano-$CaCO_3$ (100/15) composites such as PVC/($CaCO_3$/ACR), PVC/($CaCO_3$-ACR2), PVC/($CaCO_3$-PMMA/ACR), and PVC/($CaCO_3$–PMMA–ACR2).

effective load-bearing cross section areas owing to the introduction of the filler into the matrix.

To evaluate the interfacial interactions in the composites studied here, eq. (1) could be rearranged as follows:

$$\ln\{(\sigma_c/\sigma_m)[(1 + 2.5\varphi_f)/(1 - \varphi_f)]\} = B_\sigma\varphi_f \quad (2)$$

According to eq. (2), the parameter B_σ was obtained and used for evaluating interfacial interaction quantitatively. The data listed in Table III show that the interfacial interaction of PVC/($CaCO_3$–PMMA–ACR2) is the strongest due to the surface treatment of $CaCO_3$ particles and the formation of core-shell structured particles. The interfacial interaction in PVC/($CaCO_3$/ACR) is comparatively the weakest.

The interfacial interaction of polymer composites can also be evaluated by dynamic mechanical analysis (DMA).[23,24] It is well accepted that the increase of the interfacial interaction between polymer matrix and filler particles results in increase of the damping force for molecules motion, so the loss modulus and the loss factor (tan δ) of polymer composites would increase. The stronger the interfacial interaction, the higher the loss modulus and the tan δ of polymer composites. In Figures 5 and 6, the DMA results are shown. The tan δ and the loss modulus of various PVC/nano-$CaCO_3$ composites were higher than those of PVC and the order of the tan δ and the loss modulus are PVC/($CaCO_3$–PMMA/ACR) > PVC/($CaCO_3$/ACR) > PVC and PVC/($CaCO_3$–PMMA–ACR) > PVC/($CaCO_3$–ACR) > PVC. The height and area of glass transition

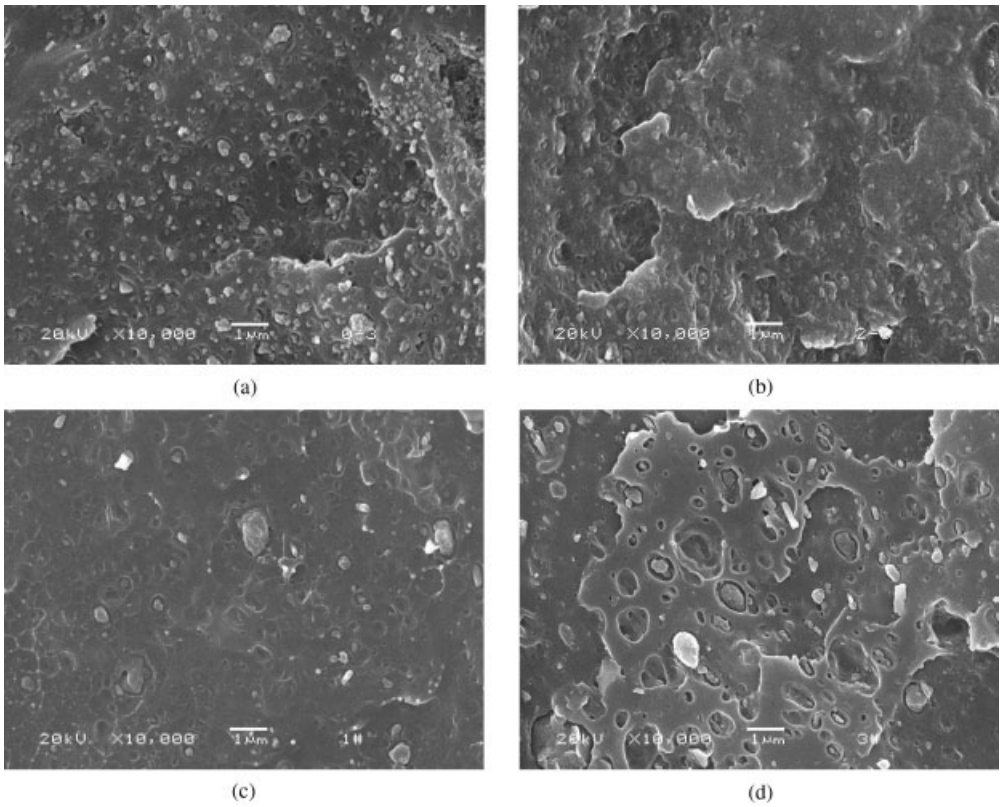

Figure 7 SEM micrographs of brittle-fractured surfaces of impact samples of PVC/$CaCO_3$ (100/15)composites: (a) PVC/($CaCO_3$/ACR), (b) PVC/($CaCO_3$_ACR2), (c) PVC/($CaCO_3$–PMMA/ACR), and (d) PVC/($CaCO_3$–PMMA–ACR2).

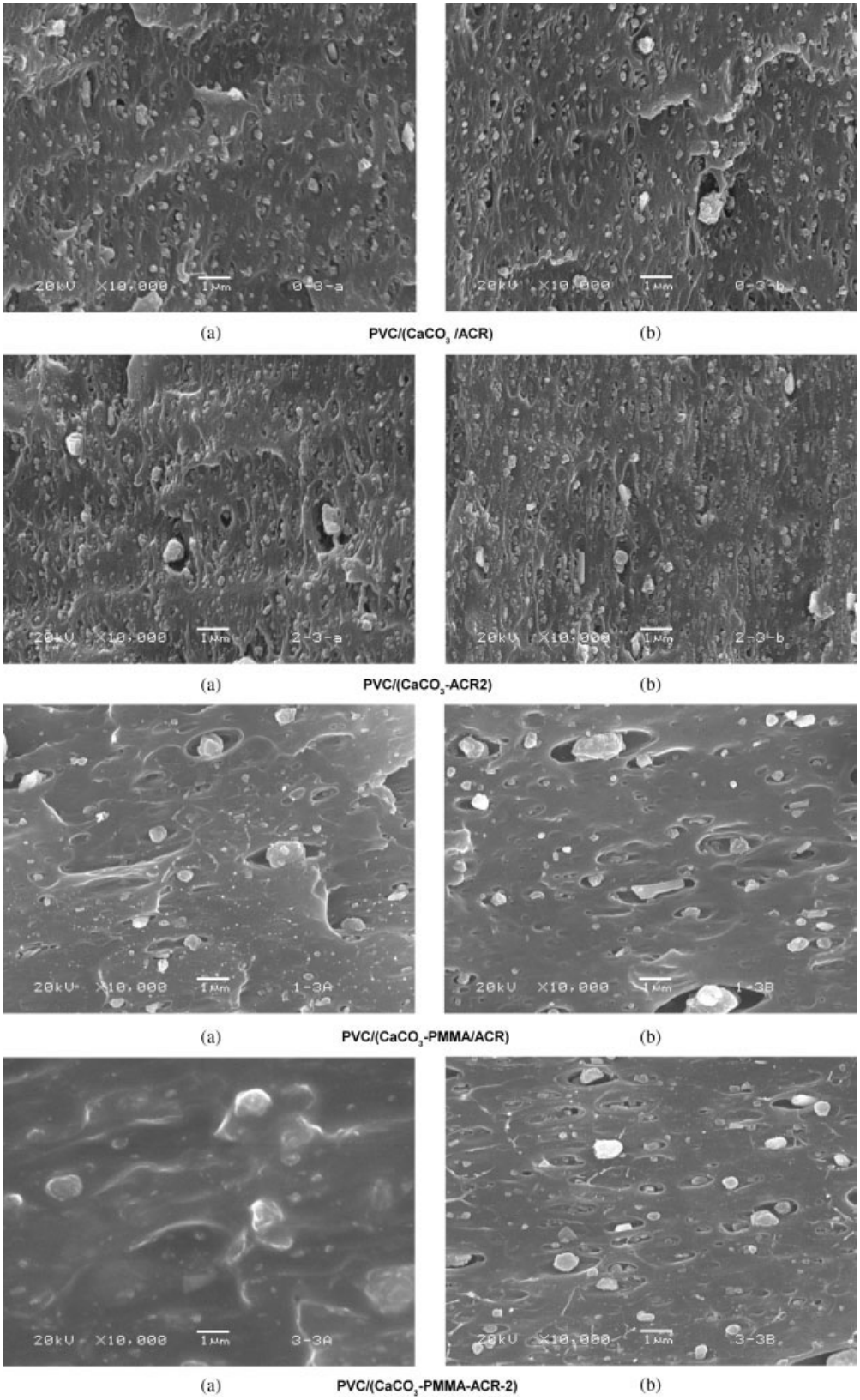

Figure 8 SEM micrographs of brittle-fractured surfaces of tensile samples of PVC/nano-$CaCO_3$ (100/15)composites along the stretching direction (a, apart from the breakpoint; b, close to the breakpoint).

peak of PVC/($CaCO_3$–PMMA–ACR) are the biggest among PVC and various PVC/nano-$CaCO_3$ composite. All these indicate that the interfacial interaction between PVC and nano-$CaCO_3$ particles can be improved by modification of nano-$CaCO_3$ particles surfaces with PMMA and formation of core-shell structured particles.

Morphology and tensile fracture behavior of various PVC/nano-$CaCO_3$ composites

Morphology of impact samples of PVC/nano-$CaCO_3$ composites was shown in Figure 7. There are many exposed $CaCO_3$ particles in PVC/($CaCO_3$/ACR) composite. But in PVC/($CaCO_3$–ACR2) and PVC/($CaCO_3$–PMMA/ACR) composites the $CaCO_3$ particles are almost wrapped by organic compounds. All these indicated that ACR was compatible with PVC but not compatible with $CaCO_3$ particles at the absence of PMMA, so when ($CaCO_3$/ACR) particles were blended with PVC, ACR was well blended with PVC and $CaCO_3$ particles were directly dispersed into PVC matrix with quite poor interfacial interaction. When $CaCO_3$–ACR2 particles were blended with PVC, $CaCO_3$ particles wrapped with ACR were well dispersed into PVC matrix, so there were almost no exposed $CaCO_3$ particles in PVC/($CaCO_3$–ACR2) composite. After $CaCO_3$ particles were treated with PMMA, ACR acted as a compatibilizer between $CaCO_3$–PMMA and PVC and so $CaCO_3$ particles were well wrapped by polymer matrix. For PVC/($CaCO_3$–PMMA–ACR2) composite, there was a good interface between $CaCO_3$–PMMA–ACR2 particles and PVC, indicating that here ACR was not completely mixed with PVC and acted as a cushion between PVC and $CaCO_3$, which can result in improvement of the mechanical properties of PVC/$CaCO_3$ composite.

Figure 8 shows the tensile fracture behaviors of various PVC/nano-$CaCO_3$ composites. There are many exposed $CaCO_3$ particles in PVC/($CaCO_3$/ACR) and PVC/($CaCO_3$–ACR2) composites both close to and apart from the breakpoint, but the filler particles in PVC/($CaCO_3$–ACR2) composite are apparently more compact with PVC matrix than in PVC/($CaCO_3$/ACR) composite. For PVC/($CaCO_3$–PMMA/ACR) composite, the $CaCO_3$ particles are almost wrapped by organic compounds in impact fractured SEM micrograph but exposed in tensile fractured SEM micrograph, indicating that interfacial interaction of PVC/($CaCO_3$–PMMA/ACR) composite was improved but not strong enough. Comparing with PVC/($CaCO_3$–PMMA/ACR) composite, the filler particles in PVC/($CaCO_3$-PMMA-ACR-2) composite were well wrapped in PVC matrix apart from the breakpoint and more compact with PVC matrix close to the breakpoint, indicating that interfacial interaction between $CaCO_3$–PMMA–ACR-2 particles and PVC was strong enough not to be destroyed before a higher critical stress was reached, or stress can be transferred to the filler particles. All these proved that interfacial interaction can be improved by modification of nano-CaCO3 particles surface with PMMA and formation of core-shell structured particles with elastic ACR shell.

CONCLUSIONS

XPS, TEM, and dissolving experiment results indicate that [($CaCO_3$ particle)/(elastomer)] core-shell structured particles can be obtained by vibro-milling and various nano-$CaCO_3$ particles with different interfacial layers between nano-$CaCO_3$ particles and PVC can be obtained by the methods used.

The mechanical properties of PVC/$CaCO_3$ composite were improved if $CaCO_3$ particles were first treated with PMMA and in succession coated by ACR through vibro-milling, and the calculated results of the interfacial interaction and DMA results reveal that the interfacial interaction between nano-$CaCO_3$ particles and PVC is the strongest here.

Morphology and tensile fracture behavior studies reveal that to make full use of the synergetic effect of elastomer and rigid particle, the elastomer should not be completely miscible with polymer matrix and there should be strong interfacial interaction between the elastomer and rigid particles.

References

1. Liu, Z. H.; Zhang, X. D.; Zhu, X.G.; Li, R. K. Y.; Qi, Z. N.; Wang, F. S.; Choy, C. L. Polymer 1998, 39, 5019.
2. Wong O. J.; Wootthikanokkhan J. W. J Appl Polym Sci 2003, 88, 2657.
3. Whittle, A. J.; Burford, R. P.; Hoffman, M. J. Plast Rubber Compos 2001, 30, 434.
4. Crawford, E.; Lesser, A. J. Polymer 2000, 41, 5865.
5. Nguyen, P. X.; Moet, A. J Vinyl Technol 1985, 7, 140.
6. Matuana, L. M.; Park, C. B.; Balatinecz, J. Polym Eng Sci 1998, 38, 1862.
7. Maldas, D.; Kokta, B.V. J Vinyl Technol 1993, 15, 38.
8. Ying, X..; Guangshun, C.; Shaoyun, G.; Xiaohua, L. China Plast Ind 2004, 32, 32.
9. Manhong, T.; Shaoyun, G. Polyvinyl Chloride 2003, 6, 22.
10. Jin, D.W.; Shon, K. H.; Kim, B. K. J Appl Polym Sci 1998, 70, 705.
11. Lizymol, P. P.; Thomas, S. J Mater Sci Lett 1998, 17, 507.
12. Ying, X.; Guangshun C.; Shaoyun, G.; Li, Z. Polyvinyl Chloride, to appear.
13. Michael, S.; Tha, P.; Morand, L. Polym Adv Technol 1996, 7, 425.
14. Guo, T. Y.; Tang, G. L.; Hao, G. J.; Song, M. D.; Zhang, B. H. J Appl Polym Sci 2003, 90, 1290.
15. Guo, T. Y.; Tang, G. L.; Hao, G. J.; Wang, S. F.; Song, M. D.; Zhang, B. H. Polym Adv Technol 2003, 14, 232.
16. Pan, M. W.; Zhang, L. C. J Appl Polym Sci 2003, 90, 643.
17. Sharifi-Sanjani, N.; Naderi, N.; Soltan-Dehghan, M. Mater Sci Forum 2003, 437/438, 419.
18. Xuefeng, D.; Jingzhe, Z.; Yanhua, L.; Hengbin, Z.; Zichen, W. Mater Lett 2004, 58, 3126.
19. Cleopatra, V. O.; Felica, W. J Appl Polym Sci 1986, 31, 951.
20. Masahiro, H.; Mitsumasa, K.; Shun-itsu, K. J Appl Polym Sci 2001, 82, 2849.
21. Pukanszky, B. N Polym Mater 1992, 3, 205.
22. Turcsanyi, B.; Pukanszky, B.; Tudos, F. J Mater Sci Lett 1988, 7, 160.
23. Chandan, D.; Diya, B.; Amarnath, B. J Appl Polym Sci 2002, 85, 2800.
24. Shuwen, P.; Xiuyan, W.; Lisong, D. Polym Compos 2005, 26, 37.